

CrossMark  
click for updatesCite this: *J. Mater. Chem. C*, 2015,  
3, 12394Received 18th September 2015,  
Accepted 18th November 2015

DOI: 10.1039/c5tc02984h

www.rsc.org/MaterialsC

## Pseudo-Hall effect in single crystal 3C-SiC(111) four-terminal devices

Afzaal Qamar,<sup>\*a</sup> Dzung Viet Dao,<sup>ab</sup> Jisheng Han,<sup>a</sup> Hoang-Phuong Phan,<sup>a</sup>  
Adnan Younis,<sup>c</sup> Philip Tanner,<sup>a</sup> Toan Dinh,<sup>a</sup> Li Wang<sup>a</sup> and Sima Dimitrijević<sup>ab</sup>

**This article reports the first results on the strain-induced pseudo-Hall effect in single crystal 3C-SiC(111) four-terminal devices. The impact of crystal orientation and the direction of strain on this effect has been presented. A single crystal p-type 3C-SiC(111) was grown by low pressure chemical vapor deposition and four-terminal devices were fabricated using conventional photolithography and dry etching processes. It has been observed that the pseudo-Hall effect in p-type 3C-SiC(111) is the same in [110] and [112] crystal orientations and is smaller than the pseudo-Hall effect of 3C-SiC(100) four-terminal devices due to the defects associated with the growth of 3C-SiC(111).**

Silicon carbide has attracted considerable attention in recent years for strain sensing applications in harsh environments.<sup>1–5</sup> SiC has superior mechanical properties, high thermal conductivity, a low thermal-expansion coefficient, good thermal-shock resistance, as well as chemical stability and electron affinity.<sup>6</sup> SiC exists in many polytypes, including 4H-SiC, 6H-SiC, and 3C-SiC, but 3C-SiC is the most cost effective and favorable polytype due to its compatibility with the existing Si MEMS process. 3C-SiC can be readily grown on Si wafers due to its capability for hetero-epitaxial growth on Si substrates of different crystal orientations *e.g.* (100), (110) or (111).<sup>7–9</sup> A large number of studies have been carried out on different polytypes of SiC and it has been established that SiC has a high potential for strain sensing applications in harsh environments.<sup>1–5,10–14</sup>

Most of the research on the strain sensing applications in SiC has been focused on 4H-SiC, 6H-SiC and 3C-SiC(100) two-terminal resistors, which normally suffer from several drawbacks, such as the requirement of a Wheatstone bridge and lateral diffusion during the fabrication process.<sup>15–18</sup> When compared to two-terminal resistors, four-terminal devices

are preferable because they are more thermally stable as they do not rely on any external Wheatstone bridge and can be made as small as possible.<sup>15–20</sup> In Si, Kanda *et al.* found that the offset voltage of four-terminal devices without a magnetic field varies significantly with the applied strain and it can be used as a measure of strain or stress sensing. This offset voltage is dependent upon the crystal orientation and also on the shape of the four-terminal devices. For Si based four-terminal devices a large number of studies on the offset voltage dependence have been carried out,<sup>17,21–25</sup> and in fact, the effect (called pseudo-Hall effect) has been utilized commercially in pressure sensors and force sensors.<sup>26–28</sup> The strain sensing behavior of 3C-SiC(100) four-terminal devices has also been investigated recently<sup>29,30</sup> and it has been found that the offset voltage of the four-terminal devices depends upon the crystal orientation and the device geometry.

To the best of our knowledge, to date, there has been no report on the pseudo-Hall effect in p-type 3C-SiC(111). Therefore, this paper aims to investigate the pseudo-Hall effect in single crystal p-type 3C-SiC(111) four-terminal devices. The strain was applied in two different orientations in the (111) crystal plane and the effect of the direction of the input current was also investigated.

A single crystal p-type 3C-SiC(111) was grown to a thickness of 245 nm on a Si(111) substrate by low pressure chemical vapor deposition. Precursors SiH<sub>4</sub> and C<sub>3</sub>H<sub>6</sub> were employed as sources of Si and C atoms respectively. Trimethylaluminum (TMAI) was used as a source of Al (p-type dopant) for *in situ* doping of the 3C-SiC film.<sup>31,32</sup> The epitaxial relationship of grown SiC to the Si substrate was investigated using X-ray diffraction (XRD) in  $\theta - 2\theta$  scan mode, the result is shown in Fig. 1(a). It can be confirmed from Fig. 1(a) that the single crystal 3C-SiC(111) was grown on Si(111). Fig. 1(b) shows the rocking curve of the 3C-SiC(111) peak and the observed FWHM value is 1.42°, which is reasonable for such a thin SiC film.<sup>31</sup> Atomic force microscopy was used to measure the roughness of the grown thin film (Fig. 1(c)) which showed a root mean square (RMS) roughness of 8.59 ± 0.5 nm for a scan area of

<sup>a</sup> Queensland Micro- and Nanotechnology Centre, Griffith University, Queensland, Australia. E-mail: afzaal.qamar@griffithuni.edu.au

<sup>b</sup> School of Engineering, Griffith University, Queensland, Australia

<sup>c</sup> School of Materials Science and Engineering, University of New South Wales, Australia

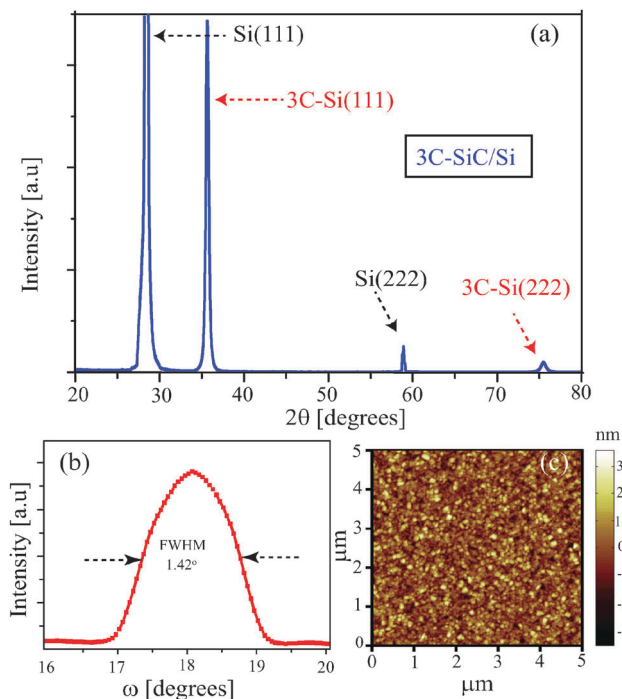


Fig. 1 (a) The XRD pattern of 3C-SiC(111) grown on Si(111); (b) FWHM of 3C-SiC(111) peak; (c) AFM image of  $5\ \mu\text{m} \times 5\ \mu\text{m}$ .

$5\ \mu\text{m} \times 5\ \mu\text{m}$ . The electrical properties of the grown film were characterized using Hall effect measurements. The carrier concentration of the p-type single crystalline 3C-SiC was found to be  $8 \times 10^{18}\ \text{cm}^{-3}$ , while the carrier concentration of the Si substrate was  $5 \times 10^{14}\ \text{cm}^{-3}$ . The resistivity of the SiC thin film was measured to be  $0.44\ \Omega\ \text{cm}$  and the hole mobility of the single crystalline 3C-SiC thin film was found to be  $1.88\ \text{cm}^2\ \text{V}^{-1}\ \text{s}^{-1}$ . Four-terminal devices were fabricated in three different orientations in the (111) plane by conventional photolithography and dry etch processes (Fig. 2(a)) to investigate the influence of crystal orientation on the strain-induced pseudo-Hall effect. Aluminum was used for depositing Ohmic contacts to the device. After fabrication of the device, the wafer was diced into strips with dimensions of  $60\ \text{mm} \times 9\ \text{mm} \times 0.625\ \text{mm}$  to apply strain using the bending beam method. The strips containing four-terminal devices were aligned in [110] and  $[11\bar{2}]$  orientations by rotating the mask during the photolithography process with respect to the reference orientation of the wafer and diced after the fabrication process.

The cantilever method in which a bending beam is used to induce strain to the fabricated devices was employed for analysis of the strain-induced pseudo-Hall effect. Fig. 2(b) shows the experimental setup for inducing the strain to the fabricated devices in which one end of the beam with the devices was fixed, while the other end was bent by a known force. The bi-layer model has been used to calculate the strain induced in 3C-SiC devices on a Si beam. The method that is used to numerically calculate the strain induced into the 3C-SiC layer on a Si strip has already been reported.<sup>2</sup> The compressive and tensile strains applied to the SiC layer were in the range

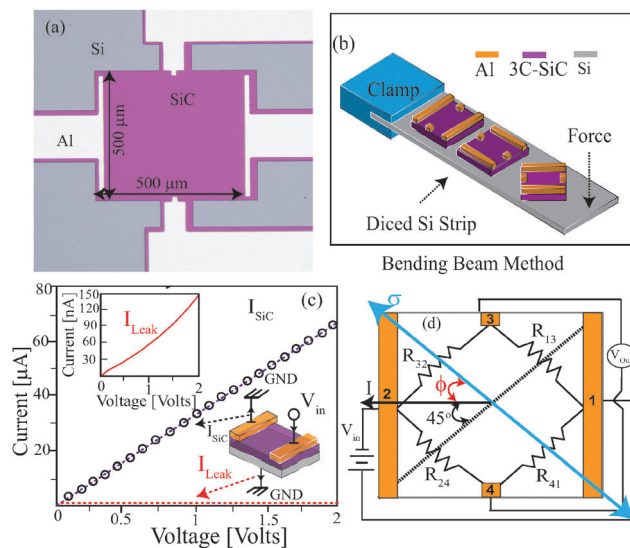


Fig. 2 (a) Microscopic image of the fabricated four-terminal device; (b) bending beam experiment to induce strain into the three SiC four-terminal devices, which are arranged in three different orientations relative to the applied strain; (c) Ohmic behavior of the contacts and the inset shows leakage current; and (d) equivalent circuit model: the strain angle  $\phi$  between the strain direction and the direction of current is also shown.

of  $-800\ \text{ppm}$  to  $800\ \text{ppm}$ . The Ohmic behavior of the Al contacts (Fig. 2(c)) and the leakage of current from 3C-SiC(111) to the Si substrate (inset of Fig. 2(c)) were also investigated to confirm that the leakage does not contribute to the measurements. Good Ohmic contacts were confirmed and the leakage current was less than 1.0% of the total current flowing through the device which is negligible. This is due to the fact that a large valence band offset between p-Si and p-3C-SiC (1.7 eV) prevents the leakage current through the SiC/Si junction.<sup>33</sup> Fig. 2(d) shows the equivalent circuit diagram of the fabricated device. The input current is applied between terminals 1 and 2 while the output voltage is measured at terminals 3 and 4. When strain is applied to the device at a constant input current, an output voltage or offset voltage across terminals 3 and 4 will change with the increase of applied strain. This effect is explained below.

From the equivalent circuit shown in Fig. 2(d), it is assumed that the offset voltage  $V_{\text{out}}$  can be presented using a Wheatstone bridge type circuit consisting of  $R_{13}$ ,  $R_{41}$ ,  $R_{32}$  and  $R_{24}$ . The resistors  $R_{13}$ ,  $R_{41}$ ,  $R_{32}$  and  $R_{24}$  are variable resistances, which depend upon the applied strain and these are part of a discrete constant circuit called the square-type bridge circuit. Without strain, it is assumed that  $R_{13} = R_{41} = R_{32} = R_{24} = R_{\text{in}}$ . The output voltage of the device in terms of these resistances can be represented as<sup>23</sup>

$$V_{\text{out}} = \frac{(R_{13}R_{24} - R_{41}R_{32})}{(R_{41} + R_{24})(R_{13} + R_{32})} V_{\text{in}} \quad (1)$$

With the application of strain, the symmetry of the device will be disturbed leading to the change in offset voltage at terminals 3 and 4. For example, when a tensile strain is applied in the diagonal axis of the device (Fig. 2(c)), resistors

$R_{13}$  and  $R_{24}$  are extended in the longitudinal direction, whereas resistors  $R_{32}$  and  $R_{41}$  are extended in the transverse direction leading to different resistance changes in these resistors and, as a result, the offset voltage  $V_{out}$  is shifted. The changes in these resistance under strain  $\varepsilon$  are<sup>25</sup>

$$\begin{cases} R_{13} = R_{24} = R_{in} [1 + (\pi_l \cos^2(\phi + 45^\circ) + \pi_t \sin^2(\phi + 45^\circ)) Y \varepsilon] \\ R_{32} = R_{41} = R_{in} [1 + (\pi_t \cos^2(\phi + 45^\circ) + \pi_l \sin^2(\phi + 45^\circ)) Y \varepsilon] \end{cases} \quad (2)$$

where  $\pi_l$  and  $\pi_t$  are longitudinal and transverse piezoresistive coefficients of 3C-SiC in the direction of the applied current,<sup>34</sup>  $\phi$  is the angle between the direction of strain and the direction of the input current as indicated in Fig. 2(d) and  $Y$  is the Young's modulus of 3C-SiC. From eqn (1) and (2), the ratio of the output voltage generated at terminals 3 and 4 to the input voltage is calculated as

$$\frac{V_{out}}{V_{in}} = \frac{(\cos^2(\phi + 45^\circ) - \sin^2(\phi + 45^\circ))(\pi_l - \pi_t) Y \varepsilon}{2 + (\pi_l + \pi_t)(\cos^2(\phi + 45^\circ) - \sin^2(\phi + 45^\circ)) \varepsilon Y} \quad (3)$$

$$\cong \frac{(-\sin 2\phi)(\pi_l - \pi_t) Y \varepsilon}{2} \quad (4)$$

as  $\cos^2(\phi + 45^\circ) - \sin^2(\phi + 45^\circ) = -\sin 2\phi$  and  $(\pi_l + \pi_t)(\cos^2(\phi + 45^\circ) - \sin^2(\phi + 45^\circ)) \varepsilon Y \ll 2$ . The strain sensitivity of the device can be defined as

$$\text{Sensitivity} = S = \left| \frac{V_{out}}{V_{in}} \right| \times \frac{1}{\varepsilon} \quad (5)$$

Fig. 3 shows the ratio of the output voltage to the input voltage of the fabricated 3C-SiC(111) four-terminal device under tensile and compressive strain in the [110] and [112] directions and with three different current directions in the (111) crystal plane. It can be observed from Fig. 3 that the ratio of the output voltage to the

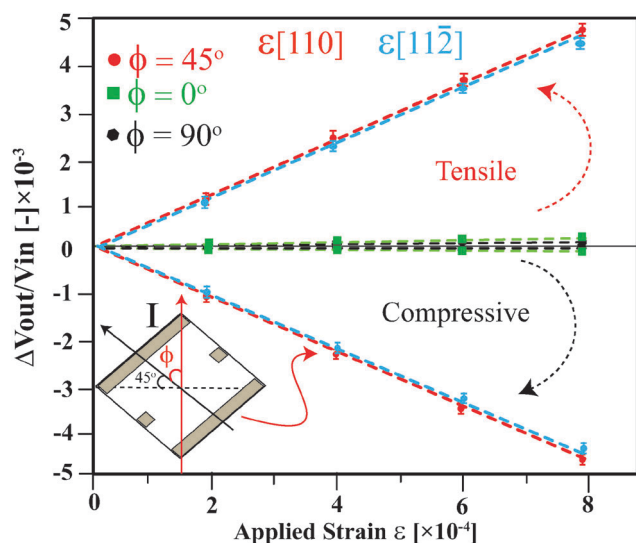


Fig. 3 The ratio of the output voltage to the input voltage of the device with varying strain in the [110] direction. The strain response of the devices with  $\phi = 0^\circ$  and  $90^\circ$  is almost negligible.

input voltage increases linearly with the applied compressive and tensile strains when the angle between the applied strain and the direction of the input current is equal to  $45^\circ$ . Eighteen devices were tested and the variation in the output voltage was less than 5%. The change in the output voltage is approximately 0 for other directions of the input current (*i.e.*  $\phi = 0^\circ, 90^\circ$ ). This is due to the fact that the change in resistances of these devices cancels each other leading to the null offset voltage change at terminals 3 and 4. In the case of  $\phi = 0^\circ, 90^\circ$ , when a tensile stress is applied to the square device for example in the [110] orientation, resistors  $R_{14}$  and  $R_{23}$  are stressed in the longitudinal direction, and so are the resistors  $R_{13}$  and  $R_{24}$ , leading to the cancellation of the piezoresistive effect in the circuit. When  $\phi = 45^\circ$ , resistors  $R_{14}$  and  $R_{23}$  are stressed in the longitudinal direction, and the resistors  $R_{13}$  and  $R_{24}$  are stressed in the transverse direction, leading to a change in the symmetry of the device (different values of piezoresistive effect in longitudinal and transverse directions) and hence an output voltage is observed at terminals 3 and 4 with applied strain.

Fig. 4 shows the output voltage of the square 3C-SiC(111) devices with the [110] and [112] strain direction and with an angle of  $\phi = 45^\circ$ . It can be observed that when a constant strain is turned on and off a repeatable signal is observed. Similarly, when the strain is gradually increased to a maximum value the output voltage increases linearly and when the strain is decreased the output voltage decreases gradually coming back to the initial value. This shows that the pseudo-Hall effect is reliable and repeatable and can be used in making strain sensing devices.

The strain sensitivities of the four-terminal devices with different strain directions in the (111) and (100) crystal planes are summarized in Table 1. It can be observed from Table 1 that at a fixed value of  $\phi$  the sensitivity of the four-terminal device in (111) is smaller than the strain sensitivity in the (100) crystal plane. The maximum achievable strain sensitivity of the four-terminal devices fabricated in the (111) plane is almost 5 times smaller than those of the four-terminal devices fabricated in the

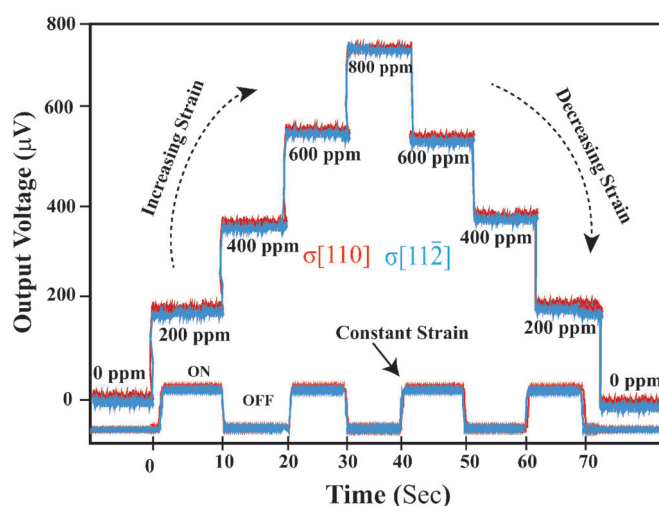


Fig. 4 Variation of the output voltage at terminals 3 and 4 with different applied strains. The input current at terminals 1 and 2 was fixed to be  $10 \mu\text{A}$ . Only the strain response of the devices with angle  $\phi = 45^\circ$  in [110] and [112] directions is given.

**Table 1** The ratio of the output voltage to the input voltage of the four-terminal devices along with strain sensitivity for different directions of strain in (111) and (100) planes. The data for 3C-SiC(100) are calculated from ref. 31

Strain direction	Plane [–]	Angle $\phi$ [degrees]	$\Delta V_{\text{out}}/\Delta V_{\text{in}}$ [ $10^{-3}$ ]	Sensitivity [–]
[110]	(111)	45°, 135°	4.81	6.0
		0°, 90°	$\approx 0$	$\approx 0$
[11 $\bar{2}$ ]	(111)	45°, 135°	4.77	5.96
		0°, 90°	$\approx 0$	$\approx 0$
[110]	(100)	45°, 135°	24.0	30
		0°, 90°	$\approx 0$	$\approx 0$
[ $\bar{1}$ 10]	(100)	45°, 135°	24.0	30
		0°, 90°	$\approx 0$	$\approx 0$

(100) plane. This is due to the fact that the growth of 3C-SiC(111) on Si(111) is associated with more crystal defects as compared to the growth of 3C-SiC(100) on Si(100). The growth of 3C-SiC(111) on Si(111) is more challenging than the growth of 3C-SiC(100) on Si(100). The defect density in 3C-SiC(100) thin film on Si(100) improves with the increase of the thickness of the film, but in the case of 3C-SiC(111) thin film growth on Si(111) the defect density is not improved with the increase of thin film thickness.<sup>35</sup> The crystal defects in 3C-SiC(111) are distributed within the whole thickness of the film and are responsible for the low mobility of the charge carriers (holes). Therefore, due to the large density of defects associated with the growth of 3C-SiC(111), the strain-induced pseudo-Hall effect in 3C-SiC(111) is smaller than the pseudo-Hall effect in 3C-SiC(100).<sup>2</sup>

The strain-induced pseudo-Hall effect in single crystal p-type 3C-SiC(111) four-terminal devices has been presented. It has been observed that the strain-induced pseudo-Hall effect in p-type 3C-SiC(111) four-terminal devices is the same in both the directions of applied strain *i.e.* [110] and [11 $\bar{2}$ ]. The pseudo-Hall effect is largest when the angle between the direction of current and applied strain is  $(2n + 1)\pi/4$  (where  $n$  is an integer). The effect is negligible when the angle between the direction of current and applied strain is  $n\pi/2$  (where  $n$  is an integer). The pseudo-Hall effect in p-type 3C-SiC(111) is smaller than the p-type 3C-SiC(100) four-terminal devices due to the crystal defects associated with the growth of 3C-SiC(111).

## Acknowledgements

This work was performed in part at the Queensland node of the Australian National Fabrication Facility, a company established under the National Collaborative Research Infrastructure Strategy to provide nano and micro-fabrication facilities for Australia's researchers. This work has been partially supported by Griffith University's New Researcher Grants.

## References

- J. Bi, G. Wei, L. Wang, F. Gao, J. Zheng, B. Tang and W. Yang, *J. Mater. Chem. C*, 2013, **1**, 4514.
- H. P. Phan, D. V. Dao, P. Tanner, N. T. Nguyen, J. S. Han, S. Dimitrijević, G. Walker, L. Wang and Y. Zhu, *J. Mater. Chem. C*, 2014, **2**, 7176–7179.
- G.-Y. Li, J. Ma, G. Peng, W. Chen, Z. Yong Chu, Y. L. He, T. Jiao Hu and X. Dong Li, *ACS Appl. Mater. Interfaces*, 2014, **6**, 22673.
- M. Mehregany, C. A. Zorman, N. Rajan and C. H. Wu, *Proc. IEEE*, 1998, **86**, 1594.
- R. Okojie, D. Lukco, V. Nguyen and E. Savrun, *IEEE Electron Device Lett.*, 2015, **36**, 174.
- J. Casady and R. Johnson, *Solid-State Electron.*, 1996, **39**, 1409–1422.
- F. L. Via, M. Camarda and A. L. Magna, *Appl. Phys. Rev.*, 2014, **1**, 031301.
- J. S. Shor, D. Goldstein and A. D. Kurtz, *IEEE Trans. Electron Devices*, 1993, **40**, 1093.
- S. Roy, C. Jacob and S. Basu, *IEEE Trans. Electron Devices*, 2003, **94**, 298.
- P. M. Sarro, *Sens. Actuators, A*, 2000, **82**, 210.
- F. Gao, J. Zheng, M. Wang, G. Wei and W. Yang, *Chem. Commun.*, 2011, **47**, 11993.
- R. Shao, K. Zheng, Y. Zhang, Y. Li, Z. Zhang and X. Han, *Appl. Phys. Lett.*, 2012, **101**, 233109.
- T. Akiyama, D. Briand and N. F. Rooij, *J. Micromech. Microeng.*, 2012, **22**, 085034.
- R. S. Okojie, A. A. Ned, A. D. Kurtz and W. N. Carr, *IEEE Trans. Electron Devices*, 1998, **45**, 785.
- R. C. Jaeger, J. C. Suhling and R. Ramani, *IEEE Trans. Compon., Hybrids, Manuf. Technol.*, 1994, **17**, 97–107.
- A. Mian, J. C. Suhling and R. Jaeger, *IEEE Sens. J.*, 2006, **6**, 340–356.
- Y. Kanda, *Jpn. J. Appl. Phys.*, 1987, **26**, 1031.
- A. V. Gridchin and V. A. Gridchin, *Sens. Actuators, A*, 1997, **58**, 219.
- M. Doelle, D. Mager, P. Ruther and O. Paul, *Sens. Actuators, A*, 2006, **127**, 261.
- R. Sunier, S. Taschini, O. Brand, T. Vancura and H. Baltesl, *Transducers, Solid-State Sensors, Actuators and Microsystems, 12th International Conference on*, 2003, **2**, 1582.
- Y. Kanda and M. Migitaka, *Phys. Status Solidi A*, 1976, **35**, K115.
- Y. Kanda and K. Yamamura, *Sens. Actuators*, 1989, **18**, 247.
- Y. Kanda and A. Yasukawa, *Sens. Actuators*, 1982, **2**, 283.
- Y. Kanda, *Sens. Actuators*, 1983, **4**, 199.
- Y. Kanda and M. Migitaka, *Phys. Status Solidi A*, 1976, **38**, K41.
- D. V. Dao, T. Toriyama, J. Wells and S. Sugiyama, *2002 15th IEEE International Conference on MEMS*, 2002; pp. 312–315.
- J. C. Doll and B. L. Pruitt, *Piezoresistor design and applications*, Springer, New York, 2013.
- J. Gragg, *Silicon pressure sensor, US Patent 4317126*, 1982.
- A. Qamar, H.-P. Phan, D. Dao, P. Tanner, T. Dinh, L. Wang and S. Dimitrijević, *IEEE Electron Device Lett.*, 2015, **1**.
- A. Qamar, P. Hoang-Phuong, J. Han, P. Tanner, T. Dinh, L. Wang, D. V. Dao and S. Dimitrijević, *J. Mater. Chem. C*, 2015, **3**, 8804–8809.
- L. Wang, A. Iacopi, S. Dimitrijević, G. Walker, A. Fernandes, L. Hold and J. Chaia, *Thin Solid Films*, 2014, **564**, 39–44.

- 32 L. Wang, S. Dimitrijević, J. Han, P. Tanner, A. Iacopi and L. Hold, *J. Cryst. Growth*, 2011, **329**, 67–70.
- 33 A. Qamar, P. Tanner, D. V. Dao, H.-P. Phan and T. Dinh, *IEEE Electron Device Lett.*, 2014, **35**, 1293–1295.
- 34 H. P. Phan, D. V. Dao, P. Tanner, N. T. Nguyen, L. Wang, Y. Zhu and S. Dimitrijević, *Appl. Phys. Lett.*, 2014, **104**, 111905.
- 35 P. Tanner, L. Wang, S. Dimitrijević, J. Han, A. Iacopi, L. Hold and G. Walker, *Sci. Adv. Mater.*, 2014, **6**, 1–6.